



An Experimental and Theoretical Studies Wings Piles at Different Sandy Soil Densities

Taha K. Mahdi, Mohammed. A. Al-Neami* , Falah H. Rahil 

Civil Engineering Dept., University of Technology-Iraq, Alsina'a street, 10066 Baghdad, Iraq.

*Corresponding author Email: 40008@uotechnology.edu.iq

HIGHLIGHTS

- The final lateral applied load is proportional to the relative density increase at the same length to diameter ratio (L/D).
- When the load is low, the wing efficiency is highest, and when the load is large, the wing efficiency drops.
- Increasing the wing length would significantly increase the pile's lateral capacity compared to the standard pile.
- Increasing sand density from loose to medium, then dense, affects the bending moment significantly. It enhanced the bending moment's magnitude.

ARTICLE INFO

Handling editor: Wasan I. Khalil

Keywords:

Lateral Load; Winged Pile; Relative Density; Slenderness Ratio; Plaxis-3D.

ABSTRACT

Increasing the cross-sectional area of the piles or adding wings to the piles are two strategies for increasing the bearing capacity of the piles to resist lateral stresses. Small and full-scale finite element models were used to investigate the effect of adding the wings on the laterally loaded pile bearing capacity in this study. Four embedded ratios (4, 6, 8, and 10) were used with various wing dimensions and numbers. The results showed that adding wings to the pile increases the resistance to lateral loads and reduces the lateral displacement significantly. To achieve the highest lateral resistance, the wings should be fixed parallel to the lateral load applied to the pile and close to the pile head. The ultimate lateral applied load is proportional to the rise in relative density. The lateral pile capacity was increased by 16.5%, 18.4%, and 33% in dense, medium, and loose sand, respectively, at the same length to diameter ratio (L/D). Increasing wing length improves lateral capacity significantly. At a failure, the lateral pile capacity was 18% and 8.5 % for Lw, equal to 112 mm and 56 mm, respectively. Another study's purpose was to determine how increasing the number of wings affected pile resistance. The lateral pile capacity at failure was increased by 9.8 % for two wings, 18.4 % for three wings, and 18 % for four wings.

1. Introduction

Piles are used to support heavy constructions subjected to lateral pressures such as heavy winds, ocean waves, hurricanes, and earthquakes, such as power transmission lines, high-rise structures, marine structures, bridge abutments, chimneys, and wind turbines [1,2]. In comparison to onshore facilities, several offshore installations are built on top of piles or are anchored with piles to facilitate transfers. In comparison to the applied vertical load, there are significant horizontal loads. As a result of these loads, the pile deflected/moved significantly, which may have resulted in serious pile failure.

A pile's lateral capacity is affected by soil type, loading direction, and pile geometry. As a result, several types of piles, such as (tapered, tripod, and helical piles), must be employed to improve pile capacity and resistance to lateral loads [3,4]. As a result, researchers have tried various strategies to enhance a pile's lateral reactivity.

The "winged-pile" concept is an innovative deep foundation technique to expand the pile's diameter, which was first proposed by Grabe et al. [5]. Other traditional approaches like increasing pile diameters have been proven to be less effective than winged or finned piles [6,7]. Wings are plates made of steel linked to the pile's outside to produce more resistance on the ground level near the surface to increase the pile's effectiveness seen in Figure 1. In addition, the pile's bearing capacity will be increased by the wings (fins), allowing the pile to be utilized in deeper water or allowing the designer to lower the size of the pile to save cost on steel and manufacturing [8].

The following are the main objectives of this investigation:

- 1) Investigating the performance of winged piles in sandy soil under lateral loads.
- 2) The influence of sandy soil density on the behavior of a laterally loaded pile is being investigated.
- 3) The impact of the length to diameter ratio (L/D) on the behavior of winged piles is being investigated.
- 4) The effect of wing size and several winged pile behavior under lateral loads is being investigated.

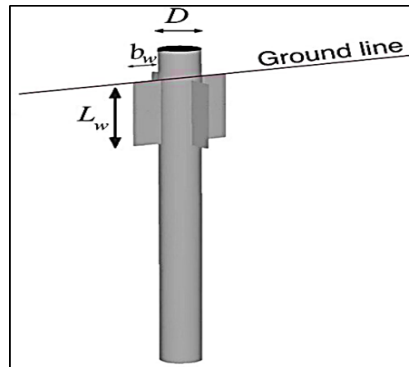


Figure 1: Winged Pile

2. Methodology

2.1 Characterization of the Soil

Dry sand is used in this study. Several tests are carried out to establish the physical and mechanical properties (specific gravity, sieve analysis, direct shear test, and maximum and minimum dry unit weight). The scale effects are taken into account, and the particle size effect is eliminated according to the recommendation suggested by Taylor [9] or a small model that states that the D/D_{50} ratio is the diameter of the pile to particle diameter at passing 50% must be not less (100). So, the D/D_{50} ratio of 142.8 is used to satisfy the requirement. Three states of sand are used (dense, medium, and loose). The characteristics of the soil are utilized in Table 1, and Figure 1 demonstrates the grain size distribution.

Table 1: Properties of the river sand used

Property	Value	ASTM Standard
Specific gravity (G_s)	2.67	D 854 [10]
D_{10} D_{30} D_{50} D_{60} (mm)	0.15, 0.23, 0.35, 0.48	
Coefficient of uniformity, (C_u)	3.2	
Coefficient of curvature, (C_c)	0.73	D 422 and D 2487
USCS Soil classification	SP	
Maximum dry unit weight [kN/m^3]	17.7	D 4253 [11]
Minimum dry unit weight [kN/m^3]	15.0	D 4254 [11]
Void ratio, (e_{max})	0.6	-----
Void ratio, (e_{min})	0.37	-----
Natural dry unit weight at R.D = 30, and 60% [kN/m^3]	15.7 and 16	
friction angle at R.D = 30, and 60%	34.7o, and 36.5	D 3080 [12]

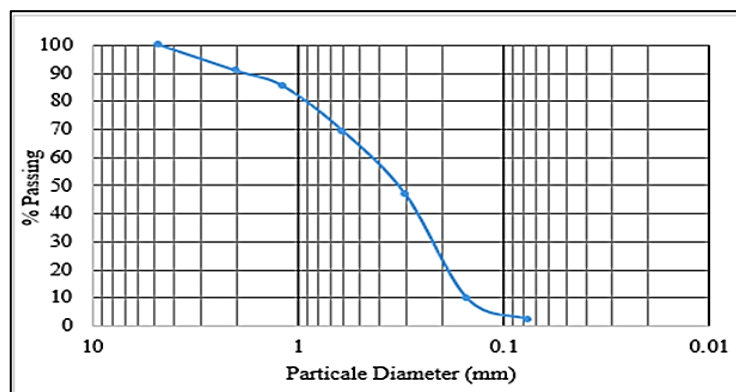


Figure 2: The grain size distribution

2.2 Wings and Model Piles

A closed-ended hollow steel winged pile model was employed. It has a 50 mm outside diameter and a 2 mm wall thickness, as mentioned in Table 2.

Table 2: Properties of model piles and wings

Parameter	Small Scale	Full Scale
Material	Steel	Steel
Modulus of elasticity, [Gpa]	200	200
Pile embedded length [mm]	200 , 300 , 400 , 500	40
Outer diameter [mm]	50	4
Wall thickness [mm]	2	50
Wing length (Lw) [mm]	56 , 112	1000, 2000
Wing width (bw) [mm]	37	2000
Wing thickness [mm]	2	50

3. 3. Program and Strategy For Testing

According to Table 3, several wing dimensions and numbers features were examined using a parametric study to see how they affect the pile's lateral capacity. The reference piles and winged piles were analyzed. Wings were constructed at the head of the pile and perpendicular to the applied static loading direction.

Table 3: small-scale model piles and wings parameters

Pile type	Pile length [mm]	Wing number	Wing length [mm]	Pile type	Pile length [mm]	Wing number	Wing length [mm]
RP20	200	-	-	WP3..30..56	300	3	56
RP30	300	-	-	WP3..30..112	300	3	112
RP40	400	-	-	WP3..40..56	400	3	56
RP50	500	-	-	WP3..40..112	400	3	112
WP2..20..56	200	2	56	WP3..50..56	500	3	56
WP2..20..112	200	2	112	WP3..50..112	500	3	112
WP2..30..56	300	2	56	WP4..20..56	200	4	56
WP2..30..112	300	2	112	WP4..20..112	200	4	112
WP2..40..56	400	2	56	WP4..30..56	300	4	56
WP2..40..112	400	2	112	WP4..30..112	300	4	112
WP2..50..56	500	2	56	WP4..40..56	400	4	56
WP2..50..112	500	2	112	WP4..40..112	400	4	112
WP3..20..56	200	3	56	WP4..50..56	500	4	56
WP3..20..112	200	3	112	WP4..50..112	500	4	112

Note: All wings have the same width = 37 mm

Total Number of Tests = 84

(28 Tests) Loose, (28 Tests) Medium and (28 Tests) Dense

RP: Reference Pile, WP: Winged Pile

WP2..50..112: Two Wings, Embedded Length 50cm, Wing Length 112 mm

4. Finite Element Mesh and Boundary Conditions

The soil and pile were simulated using finite element modeling (PLAXIS 3D), allowing for a full examination of the interaction between soil and structure. The sandy soil was designed to be a flexible linear elastic substance. To predict nonlinear sand behavior, the Mohr-Coulomb material model was utilized due to its clarity, simulating issues in pile behavior subjected to lateral stresses with a sufficient number of model parameters and appropriate precision. Piles placed laterally on sandy soil under dry conditions are examined to match the standard and wing pile situations. There are five main input parameters in the Mohr-Coulomb model: elasticity modulus (E), internal friction angle (ϕ), dilatancy (ψ), Poisson's ratio (ν), and cohesion (c).

The friction angles were calculated using the direct shear test data in the loose, medium, and dense states. The elasticity modulus was estimated using the results of the direct shear [13]. The dilatancy angle (ψ) was calculated using the equation published by using the PLAXIS program for soil-type quartz sand ($\psi = \phi - 30^\circ$). In the analysis, the value of (c) was zero. The initial stress in the numerical simulation was generated using the earth pressure coefficient at rest $K_0 = 1 - \sin$ according to the Jaky formula [14]. The hyperbolic model parameters utilized in the study are listed in Table 4, and the mesh was set to medium (element: 8448 and node:13851). The pile model is tethered in the middle of sand [15], as shown in Figure (3).

Finally, to illustrate the interaction between the sand and the pile, an interface element was developed around the ring of the pile. When an interface element is in slip mode, the interface's shear modulus decreases. In PLAXIS, a strength reduction factor (R_{inter}) represents the fall in strength for the interface element. The interface strength reduction factor (R_{inter}) for sand is set at 0.65, which is common for sand-steel contacts [16]. This factor connects the interface properties to the soil layer's strength properties in the following way:

$$\tan \phi_{inter} = R_{inter} \tan \phi_{soil} \tag{1}$$

$$c_{inter} = R_{inter} c_{soil} \tag{2}$$

$$\psi_{inter} = \begin{cases} 0 \cdot 0 & \text{if } R_{inter} < 1 \\ \psi_{soil} & \text{otherwise} \end{cases} \tag{3}$$

ϕ_{inter} , c_{inter} , and ψ_{inter} are the interface's friction, cohesion, and dilatancy angles, respectively.

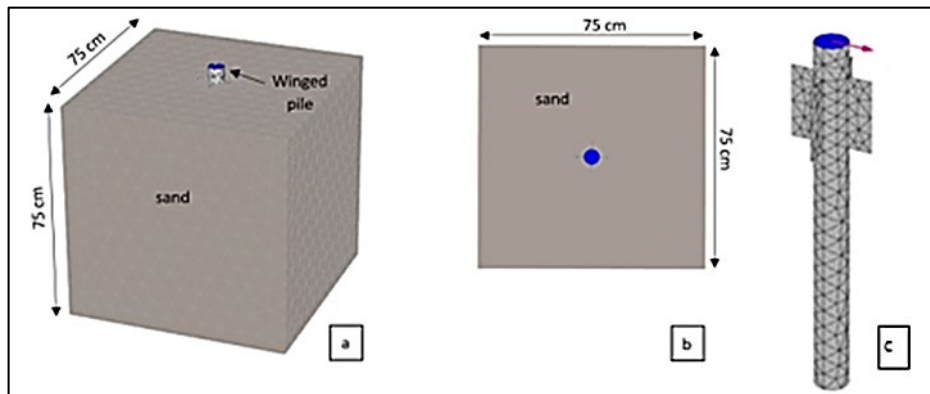


Figure 3: The lateral loaded winged pile model

Table 4: The characteristics of the materials used in (PLAXIS-3D)

Parameter	Loose Sand Dr=35%	medium Sand Dr=60%	Dense Sand Dr=75%	Pile and Wings
Material Model	Mohr-Coulomb soil model	Mohr-Coulomb soil model	Mohr-Coulomb soil model	Linear elastic
Type of material behavior	Drained	Drained	Drained	Nonporous
dry unit weight γ_d (kPa)	15.7	16	16.5	78
Effective friction angle (ϕ)	35°	37°	41°
Effective cohesive strength(c) (kPa)	0	0	0
elasticity modulus (E) (MPa)	0.75	4.4	9	200x10 ³
Poisson's ratio (ν)	0.33	0.33	0.33	0.3
Dilatancy angle (ψ)	4.65	6.45	10.6
strength reduction factor (R_{inter})	0.65	0.65	0.65

5. Results of the Study

Load-displacement relationships for piles with and without wings based on finite element analysis are given below. Failure occurs when the lateral load equivalent to a lateral displacement exceeds 10% of the diameter of the pile. [17]. The most significant layer of soil around a pile is the top layer [18]. In each test series, wings were formed on top of the pile beneath the soil surface. This was the best location for increasing ultimate load capacity. The incremental acting loads are given perpendicular to the wing plan in each test series.

5.1 Verification Between Numerical and Experimental Results

A numerical model was compared to the results of laboratory testing on laboratory scale piles to view the analysis procedure to give an acceptable result. In addition, the head of the pile load-displacement curves was compared to a model test utilizing PLAXIS-3D computational assessments of a winged pile, revealing that the numerical technique may be used to estimate pile height while enhancing precision at displacements. Figure 4 shows the lateral load at the end of test 195 N and 259.6 N for RP50 and WP4..50..112 (4 wings, embedded length 50 cm, and wing length 112mm), respectively, which is similar to what the numerical studies predicted 200 N and 264.6 N for RP50 and WP4..50..112, respectively. This proves that the numerical model of winged pile behavior is acceptable.

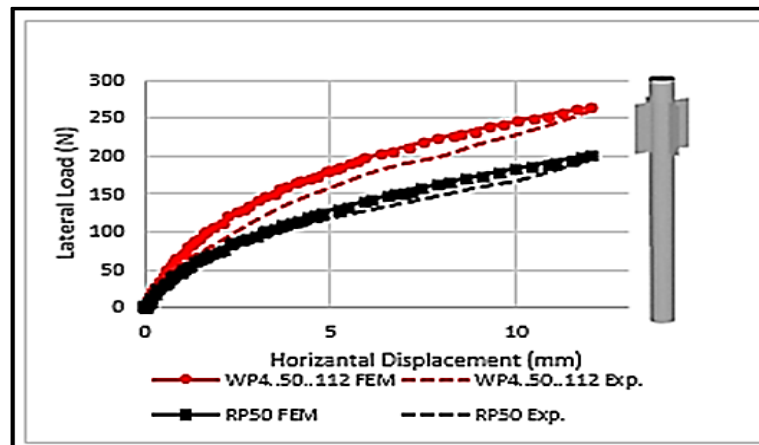


Figure 4: Lateral load versus horizontal displacement for a single winged pile model with a relative the density of 35%

5.2 Effect of Wing Length on the Lateral Capacity of Winged Pile

The wing width was kept constant throughout the tests for various wing lengths. Figure 5 illustrates the lateral load capacity and horizontal displacement curves, demonstrating that increasing wing length improves lateral capacity significantly. At a failure, the lateral pile capacity was 18% and 8.5 % for L_w , equal to 112 mm and 56 mm, respectively, with $L/D = 10$, relative density equal to 60 %, and three wings when compared to the reference pile. In lateral force resistance, the pile length and the wing length are important characteristics.

In reality, the most effective location for soil resistance is perpendicular to the load direction. This is because the wings' diameter and area are equivalent to the area above the wingtip of a winged pile. As a result, the area behind the wings significantly impacts the passive resistance produced.

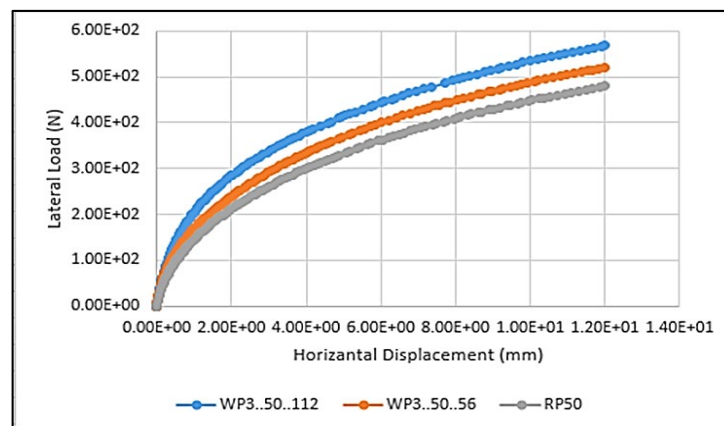


Figure 5: The load-displacement curve at different wing lengths for $L/D=10$ and Medium sand

Figure 6 shows the variation of bending moment in piles, RP50 and WP4..50..112, as a function of depth. The largest moment in WP4..50..112 is in the pile's midsection; there is usually no moment at the pile's head or base. Figure 7 shows the displacement of piles as a function of depth. The piles' near-rigid ground is demonstrated by the lack of significant deformation in the pile

body. Instead of deforming as the load develops, it piles in its direction. As a result, about two-thirds of the distance down the pile from the load application point is a rotation point. Figure 8 shows the pile-soil deformation.

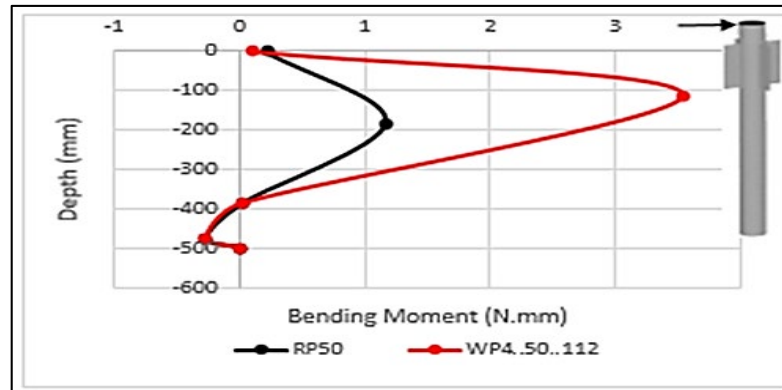


Figure 6: The Bending moment along pile for L/D= 10, with relative density = 60%

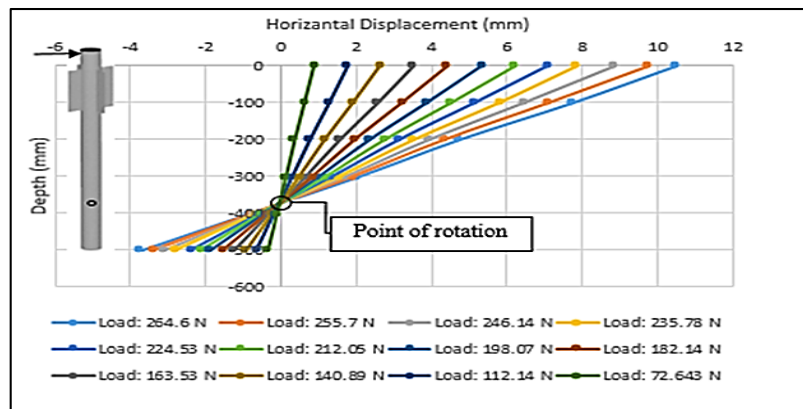
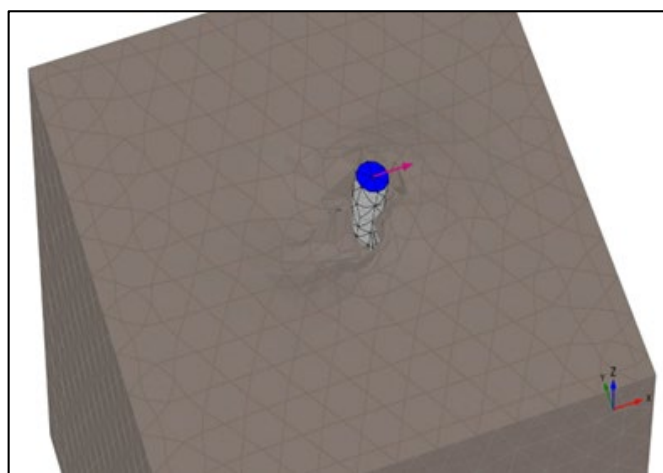


Figure 7: Variation of lateral displacement with depth WP4..50..112 at relative density 35%

5.3 Effect of Wings Number on the Lateral Capacity of Winged Pile

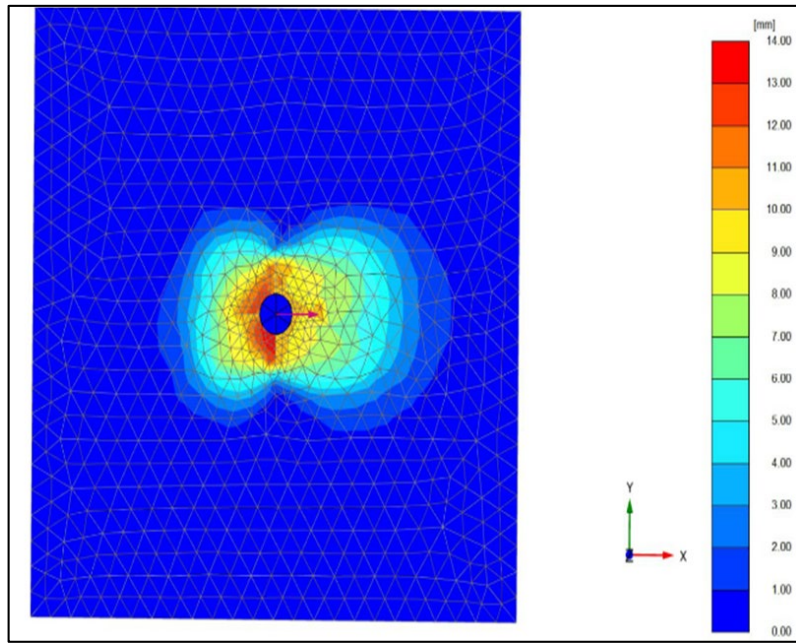
Another study's purpose was to determine how increasing the number of wings affected pile resistance at $L_w=112$ mm and $Dr=60$ percent. The load-displacement curves show that as the number of wings rises, the pile capacity against lateral force increases, as shown in Figure 9.

Compared with the reference pile for pile stiffness, the lateral pile capacity at failure was increased by 9.8 % for two wings, 18.4 % for three wings, and 18 % for four wings.

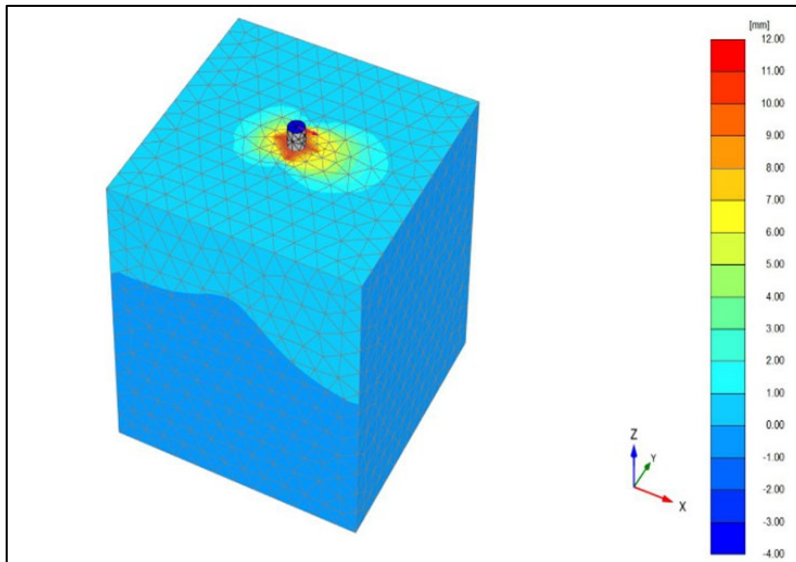


(a)

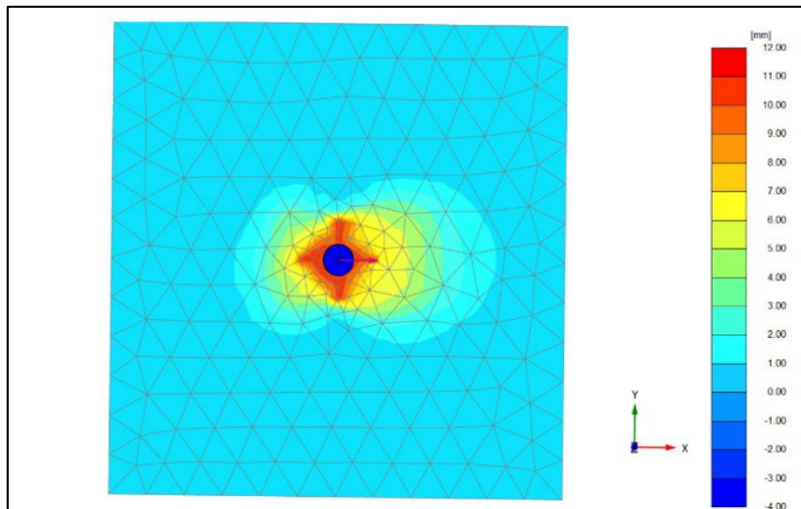
Figure 8: Pile- soil deformation (a and b) total lateral displacement (c and d) lateral displacement for x-direction only



(b)



(d)



(c)

Figure 8: Continued

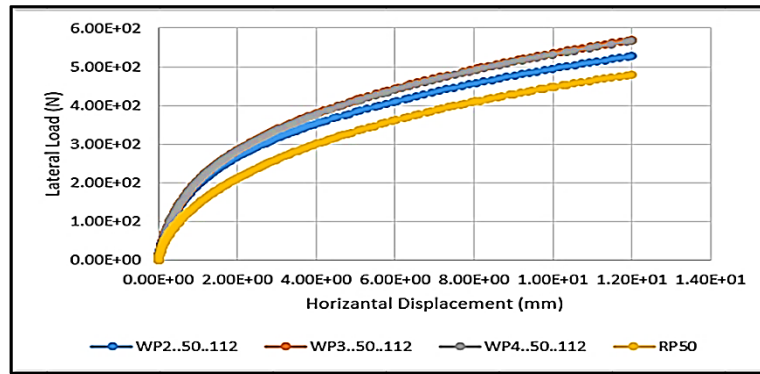


Figure 9: The curves of load-displacement for different Wing Numbers at L/D= 10 and medium relative density

5.4 Effect of Slenderness Ratio L/D On the Lateral Capacity of Winged Pile

The slenderness ratio (L/D) of the piles is varied (4, 6, 8, and 10) to show the wing's efficiency in short and long piles [19,20]. The slenderness ratio greatly enhances the load-carrying capability of winged piles, as demonstrated in Figure 10. The higher the (L/D) ratio, the greater the gain in lateral capacity. At a failure, the lateral pile capacity was increased by 18.4 % for L/D=10, 24.6 % for L/D=8, 30.4 % for L/D=6, and 40.5 % for L/D=4 when comparing the winged pile to a reference pile.

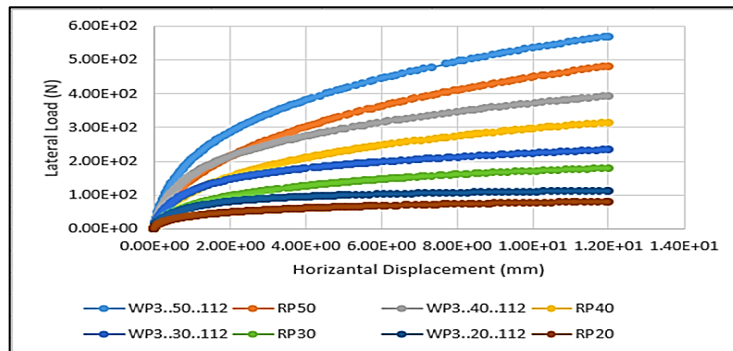


Figure 10: Load-displacement curves for different slenderness's ratios (10, 8, 6, 4) at a medium relative density

5.5 Effect of Relative Density on The Lateral Capacity of Winged pile

As demonstrated in Figure 11, the relative density, D_r , impacts the lateral load of winged piles. A better lateral load capability is correlated with higher relative density [21]. This is since, as the sand becomes denser, its shear strength increases[22,23]. For wing length of 112 mm with three wings, length to diameter ratio (L/D =10), and at a failure, the lateral pile capacity was increased by 16.5%, 18.4%, and 33% in dense, medium, and loose sand, respectively.

5.6 Full-Scale Modelling

The elastic soil parameters relating to medium sand were examined in the full scale investigation.: dry unit weight (γ_d) = 16 kN/m³, Poisson's ratio (ν) = 0.33, dilatancy angle (ψ) = 6.45, effective friction angle (ϕ) = 36.45, elasticity modulus (E) = 40 MPa, and effective cohesive strength c = 0 kPa.

The barrier is a cube with sides 22.5 times the pile's diameter and a depth 2.5 times the pile's length. As long as there was no bottom boundary, the 'ground surface' was free to travel in any direction. However, as a safety measure, the vertical boundaries were anchored in place to prevent movement in the opposite direction[24].

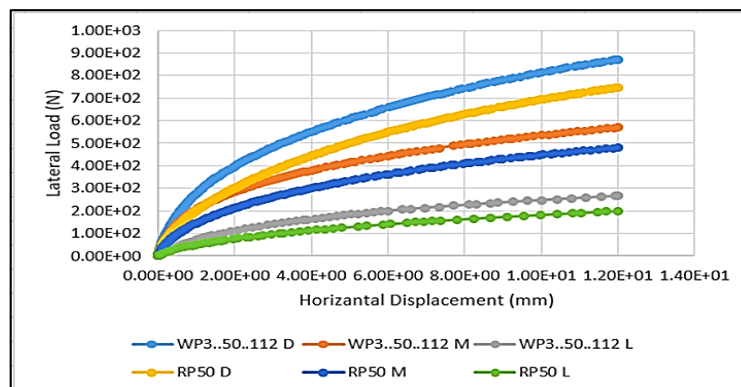


Figure 11: load-displacement curve in various Relative densities ($D_r=35, 60$ and 75%)

5.7 The Behavior of A Full-Scale Winged Pile

One of the objectives of this study was to understand the pile-soil interaction of wing piles better. The full-scale winged pile was subjected to a lateral load during the computer modeling process. The use of the typical Mohr-Coulomb model is justified in this case. It should be mentioned that the purpose of this simulation was to demonstrate the possible advantages of using wing piles as a full-scale foundation. Figure 12 illustrates the surface deformation of the pile and soil. Figure 13 shows the lateral load at the end of the test 36 MN, 42 MN, and 47 MN for RP40, WP4..40..10(4 wings, embedded length 40 m and wing length 10m) and WP4..40..20(4 wings, embedded length 40 m and wing length 20m), respectively. At a failure, the lateral pile capacity was increased 16 % for WP4..40..10 and 30% for WP4..40..20 when compared with the reference pile.

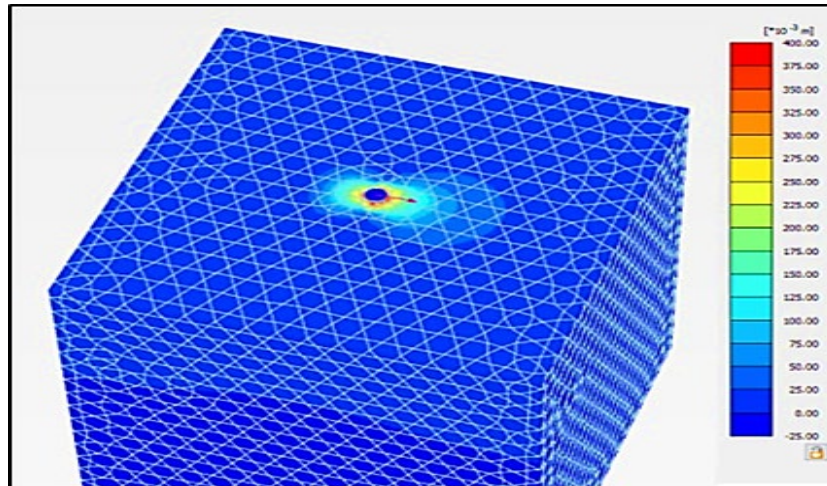


Figure 12: Pile- soil deformation full scale

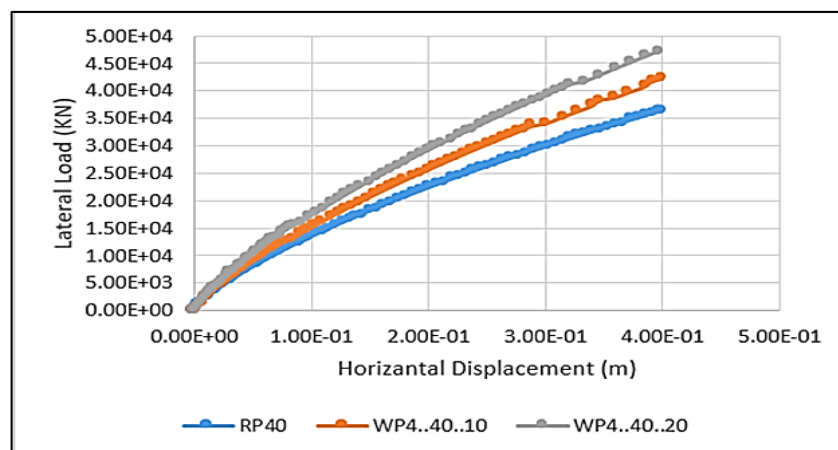


Figure 13: Load-displacement curves for a full-scale winged pile model with a relative density of 60%

6. Conclusion

The following points can be summarized based on the collected data and after comparing the winged pile to those of the reference pile, as well as assessing the objectives to determine the ideal settings for optimal performance:

- 1) In the case of lateral loading, wings are directed parallel to the loads and installed close to the pile head to give better resistance.
- 2) Wing efficiency is greatest when the load is light and diminishes when the load is heavy.
- 3) The final lateral applied load is proportional to the increase in relative density when the length to diameter ratio remains constant.
- 4) The bending moment is significantly affected by increasing the sand density from loose to medium to dense. The magnitude of the bending moment increased as a result.

Author contribution

All authors contributed equally to this work.

Funding

This research received no specific grant from any funding agency in the public, commercial, or not-for-profit sectors.

Data availability statement

The data that support the findings of this study are available on request from the corresponding author.

Conflicts of interest

The authors declare that there is no conflict of interest.

References

- [1] C.-C. Fan and J. H. Long, Assessment of existing methods for predicting soil response of laterally loaded piles in sand, *Comput. Geotech.*, 32 (2005) 274–289. <https://doi.org/10.1016/j.compgeo.2005.02.004>
- [2] S. H. Reza Tabatabaiefar, B. Fatahi, and B. Samali, Seismic behavior of building frames considering dynamic soil-structure interaction, *Int. J. Geomech.*, 13 (2013) 409–420. [https://doi.org/10.1061/\(ASCE\)GM.1943-5622.0000231](https://doi.org/10.1061/(ASCE)GM.1943-5622.0000231)
- [3] M. H. El Nagggar and M. Sakr, Cyclic response of axially loaded tapered piles, *Int. J. Phys. Model. Geotech.*, 2 (2002) 1–12. <https://doi.org/10.1680/ijpmg.2002.2.4.01>
- [4] Y. V. S. N. Prasad and S. N. Rao, Lateral capacity of helical piles in clays, *J. Geotech. Eng.*, 122 (1996) 938–941. [https://doi.org/10.1061/\(ASCE\)0733-9410\(1996\)122:11\(938\)](https://doi.org/10.1061/(ASCE)0733-9410(1996)122:11(938))
- [5] J. Grabe, K. Mahutka, and J. Dührkop, Monopilegründungen von Offshore-Windenergieanlagen–Zum Ansatz der Bettung, *Bautechnik*, 82 (2005) 1–10. <https://doi.org/10.1002/bate.200590020>
- [6] A. M. A. Nasr, Experimental and theoretical studies of laterally loaded finned piles in sand, *Can. Geotech. J.*, 51 (2014) 381–393. <https://doi.org/10.1139/cgj-2013-0012>
- [7] J. Grabe and J. Dührkop, Improving of lateral bearing capacity of mono-piles by welded wings, in *Proceedings of the 2nd international conference on foundations*. HIS BRE Press, Garston, UK, 2008.
- [8] P. J. Millett, M. J. Allen, and M. P. G. Bostrom, Effects of alendronate on particle-induced osteolysis in a rat model, *J. Bone Jt. Surg.*, 84 (2002) 236–249. <https://doi.org/10.2106/00004623-200202000-00011>
- [9] R. N. Taylor, *Geotechnical Centrifuge Technology*, First ed., Chapman & Hall, London., 1995.
- [10] ASTM, Standard Test Method for Specific Gravity of Soil Solids by Water Pycnometer, ASTM D854, West Conshohocken, Pennsylvania, USA., 2006.
- [11] ASTM, Standard Test Method for Maximum Index Density And Unit Weight of Soils Using A Vibratory Table, ASTM D425300, West Conshohocken, Pennsylvania, USA., 2006.
- [12] ASTM, Standard Test Method for Direct Shear Test of Soils under Consolidated Drained Conditions, ASTM D3080-04, West Conshohocken, Pennsylvania, USA., 2006.
- [13] M. Budhu, *Soil Mechanics and Foundation*, 3rd Edition John Wiley & Sons Inc, ISBN 2010.
- [14] J. Jaky, The Coefficient of Earth Pressure at Rest, *J. Soci. Hungarian Arch. Eng.*, 1944. [https://doi.org/10.1061/\(ASCE\)1090-0241\(2005\)131:11\(1429\)](https://doi.org/10.1061/(ASCE)1090-0241(2005)131:11(1429))
- [15] M. A. Al-Neami, M. H. Al-Dahlaki, and A. H. Chalob, Effect of Embedment and Spacing Ratios on the Response of Lateral Load of Single and Group Piles, *Eng. Technol. J.*, 39 (2021) 1144–1152. <https://doi.org/10.30684/etj.v39i7.1881>
- [16] J.-R. Peng, M. Rouainia, and B. G. Clarke, Finite element analysis of laterally loaded fin piles, *Comput. Struct.*, 88 (2010) 1239–1247. <https://doi.org/10.1016/j.compstruc.2010.07.002>
- [17] Y. E. A. Mohamedzein, F. A. E. Nour Eldaim, and A. B. Abdelwahab, Laboratory model tests on laterally loaded piles in plastic clay, *Int. J. Geotech. Eng.*, 7 (2013) 241–250. <https://doi.org/10.1179/1938636213Z.00000000030>
- [18] L. Zhang, Nonlinear analysis of laterally loaded rigid piles in cohesionless soil, *Comput. Geotech.*, 36 (2009) 718–724. <https://doi.org/10.1016/j.compgeo.2008.12.001>
- [19] B. B. Broms, Lateral resistance of piles in cohesionless soils, *J. Soil Mech. Found. Div.*, 90 (1964) 123–156.
- [20] A. Boominathan, R. Ayothiraman, An experimental study on static and dynamic bending behaviour of piles in soft clay, *Geotech. Geol. Eng.*, 25 (2007) 177–189. <https://doi.org/10.1007/s10706-006-9102-7>
- [21] I. A. Ali, S. F. Abbas, and K. H. Ibrahim, Effect of the Slenderness Ratio of Piles on Ultimate Lateral Resistance in Sandy Soil, *Eng. Technol. J.*, 39 (2021) 1740–1747. <http://dx.doi.org/10.30684/etj.v39i12.105>
- [22] U. Salini, M. S. Girish, Lateral Load Capacity of Model Piles on Cohesionless Soil, *Electron. J. Geotech. Eng.*, 14 (2009) 1–11. http://dx.doi.org/10.3208/sandf.39.2_21
- [23] F. H. Rahil, M. A. Al-Neami, and K. A. N. Al-Zaho, Effect of Relative Density on Behavior of Single Pile and Piles Groups Embedded with Different Lengths in Sand, *Eng. Technol. J.*, 34 (2016) Part (A).
- [24] J. R. Peng, M. Rouainia, B. G. Clarke, P. Allan, and J. Irvine, Lateral resistance of finned piles established from model tests, *Int. Conference on Geotech. Eng.*, 2004.